0 (0000) 0 – 0

ISBN 0-9780479

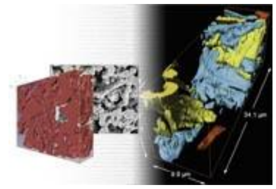

AES-ATEMA' 2011 International Conference on Advances and Trends in Engineering Materials and their Applications
(Milan, Italy: July 04 - 08, 2011)

Aeroelastic Analysis of Wind Turbines Using Free General-Purpose Multibody Dynamics Software

Mohamed W. Mehrez [1], Ayman A. El-Badawy [2]*

[1] Dept. of Mechatronics Engineering, German University in Cairo, Cairo, Egypt
(Email: mohamed.waleed@guc.edu.eg)

[2] Dept. of Mechanical Engineering, Al-Azhar University, Cairo, Egypt and Dept. of Mechatronics Engineering, German University in Cairo, Cairo, Egypt
(Email: ayman.elbadawy@ guc.edu.eg)

*Corresponding Author

Abstract

In this paper, a free general-purpose multibody dynamics code is used to analyze the aeroelastic behaviour of the control advanced research wind turbine. The wind turbine model has been built up with beam elements, joints, aerodynamic elements. An impulsive wind is applied to the turbine rotor plane. The blade and tower natural frequencies are obtained. Steady and unsteady wind speeds are then applied. A couple which is a function of the rotor angular velocity is applied at the rotor horizontal revolution hinge to counteract the aerodynamic torque. Simulation results are then obtained, presented and discussed in terms of the variation of blade tip deflection (flap wise, edgewise, and torsional) as a function of time together with its effect on the output power.

Keywords

Wind turbine, aeroelastic analysis, multibody dynamics, open source code, structural dynamics.

1 Introduction

The design of high-performance wind turbines requires high fidelity analysis of the system behavior including the interaction of its aspects like structural dynamics, aerodynamics, power generation and control. To ensure that designers explore different architectures and design details, the analysis tools must be versatile and flexible. Unlike the commercial softwares doing wind turbine aeroelastic simulation, the free/open source analysis tools give the designers more flexibility to solve their own special design problems by modifying the source codes [1].

There have been various methods in structural modeling over the past several decades. Firstly, the assumed mode shape method [2] is very popular in the wind energy industry due to its low computational cost and can provide a compact system matrix for control design. However, this type of approach is not sufficient for the detailed design of the wind turbines, especially for the large diameter rotors with flexible blades. Finite Element Method (FEM) could produce more detailed results for these problems, but at high computational cost. Thus, a method based on flexible, non-linear multi-body dynamics may become a good choice [3]. This work utilizes a free general-purpose multibody dynamics software MBDyn [4] to analyze the aeroelastic behavior of the control advanced research wind turbine using general purpose elements, such as, beam elements, joints, aerodynamic elements and control system components.

2 Wind Turbine Description

The reference wind turbine used in the simulations is the Controls Advanced Research Turbine (CART0) which is a machine rated at 600 kW. The CART0 is fitted with an induction generator, rigid coupling, and individual electromechanical pitch actuators. The rotor runs upwind of the tower and consists of two blades and a teetering hub [5].

2.1 Wind turbine model assembling and description

In order to use MBDyn to do time domain calculation on a wind turbine, a model has to be built up with beam elements, joints, aerodynamic elements which are provided by the code. In MBDyn, the reference wind turbine system is modeled as a deformable, elastic tower, 34.862 m high, carrying a rigid nacelle, on which a rotor is mounted with two flexible blades. The tower is modeled by five beam elements, each containing three nodes. The rotor hub is described by a rigid body element and can rotate around a horizontal revolution hinge, but at the free end of the main shaft, which is rigidly connected on the nacelle element having 3.7 degrees tilt angle. Two blades are mounted on the hub with a 0.668 meters offset from the Low Speed Shaft (LSS) coupling and with 0 degrees pre-cone angle. They are clamped on the hub while the pitch angle can be imposed. The blades have a span of 19.955 meters. They are modeled by five, three node beams. A couple which is a function of the rotor angular velocity is applied at the rotor horizontal revolution hinge to counteract the aerodynamic torque, which works as a generator torque. The blade elastic and inertial properties are varying along the spanwise position. A schematic of the overall assembling result is presented in Figure 1.

The aerodynamic model in MBDyn is Blade Element Momentum (BEM) theory with tip-root loss correction [6]. In this paper, at the same blade radius position in the rotor plane, a uniform induced velocity is considered. Standard air density at hub center height is considered, that is ρ = 1.225kg/m3. The aerodynamic forces on the blades are taken into account by means of five aerodynamic elements each one attached on each blade beam element at the middle node of the beam element. The airfoil considered along the spanwise direction of the blade is S809 which is developed for wind turbine applications.

According to NREL [7], it exhibits a maximum lift coefficient (C_{lmax}) which is relatively insensitive to roughness effects. The aerodynamic elements use the experimentally determined aerodynamic coefficients C_l, C_d and C_m to calculate the aerodynamic force on each blade.

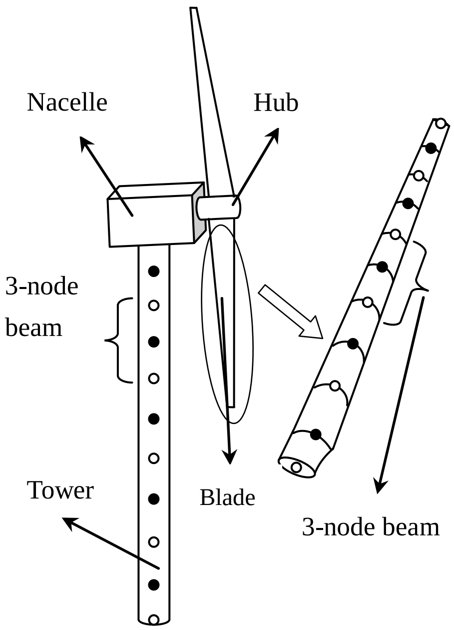

Figure 1. Structure model of wind turbine

3 Multibody Model

The multibody analysis is based on an original formulation, implemented in the free general purpose software MBDyn. It performs the direct time integration of Initial Value Problems (IVP) written as a system of first order Differential-Algebraic Equations (DAE) [8]. The equations of motion of each unconstrained body are written in first order form using the Newton-Euler approach.

The definitions of momentum, β_i, and angular momentum about the node γ_{xi}, for the *i*-th node are

$$m_i \dot{x}_i + \omega_i \times s_{ix_i} = \beta_i \quad (1)$$

$$s_{ix_i} \times \dot{x}_i + \mathbf{J}_{ix_i} \omega_i = \gamma_{ix_i} \quad (2)$$

where m_i is the mass of the node, x_i is the location of the node, ω_i is the angular velocity of the node, s_{ixi} is the static moment of the node referred to the node's location, and $\mathbf{J}_{ixi}$ is the inertia tensor of the node referred to the node's location. The equilibrium of each node yields

$$\dot{\beta}_i = \sum \mathbf{f}_i \quad (3)$$

$$\dot{\gamma}_{ix_i} + \dot{x}_i \times \beta_i = \sum \mathbf{m}_{ix_i} \quad (4)$$

where all external forces, $\mathbf{f}_i$, and moments, $\mathbf{m}_{ixi}$, acting on the node are considered. The equations of motion of all the unconstrained nodes can be summarized as

$$\mathbf{M}\dot{\mathbf{q}} = \mathbf{p} \quad (5)$$

$$\dot{\mathbf{p}} = \mathbf{f}(\mathbf{q}, \dot{\mathbf{q}}, \mathbf{p}, t) \quad (6)$$

where **q** summarizes the kinematic variables of the nodes, while **p** summarizes the momentum and angular momentum. The function **f** represents the generic configuration-dependent forces acting on the nodes. It includes the contributions related to structural deformability, significantly those related to finite-volume beam elements [9]. The constrained system dynamics are modeled by explicitly adding kinematic constraints between the nodes in form of algebraic equations, using the Lagrange's multipliers formalism. The addition of m_h holonomic and m_{nh} non-holonomic constraints, respectively expressed by $\boldsymbol{\varphi}(\mathbf{q}, t) = \mathbf{0}$ and $\boldsymbol{\psi}(\dot{\mathbf{q}}, \mathbf{q}, t) = \mathbf{0}$, result in

$$\mathbf{M}\dot{\mathbf{q}} = \mathbf{p} \quad (7)$$

$$\dot{\mathbf{p}} + \boldsymbol{\varphi}^T \boldsymbol{\lambda} + \boldsymbol{\psi}^T \boldsymbol{\mu} = \mathbf{f}(\mathbf{q}, \dot{\mathbf{q}}, \mathbf{p}, t) \quad (8)$$

$$\boldsymbol{\varphi}(\mathbf{q}, t) = \mathbf{0} \quad (9)$$

$$\boldsymbol{\psi}(\mathbf{q}, \dot{\mathbf{q}}, t) = \mathbf{0} \quad (10)$$

where $\boldsymbol{\lambda}$ and $\boldsymbol{\mu}$ respectively are the multipliers related to the holonomic and non-holonomic constraints. The implicit DAE problem of the system assumes the form.

$$\mathbf{g}(\mathbf{y}, \dot{\mathbf{y}}, t) = \mathbf{0} \quad (11)$$

where $\mathbf{y} = [\mathbf{q}^T, \mathbf{p}^T, \boldsymbol{\lambda}^T, \boldsymbol{\mu}^T]^T$ summarizes all the variables of Eq. (8). Eq. (11) is solved using a Newton-Raphson technique.

4 Modal Analysis

An impulsive wind speed is applied to the rotor plane of the turbine model. The impulse input is shown in Figure 2. Figure 3 shows the frequency spectrum of blade flapwise and blade tip torsional deformation. For flapwise deformation, the first mode is observed to be at 2.096 Hz. For blade tip torsional deflection, the first mode is observed to be at frequency of 11.09 Hz.

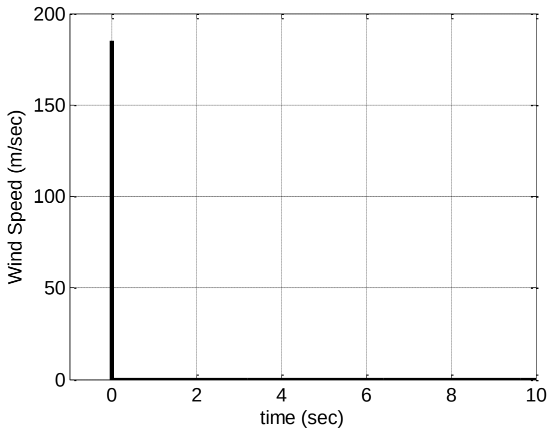

Figure 2. Impulse input

Figure 4 shows the spectrum of tower fore-aft deflection, where the first mode is observed to be at 0.898 Hz. The tower lateral deflection is observed to be of the same natural frequency as the fore-aft deflection. This is due to the fact that the cross section of the tower top is symmetric.

The results obtained are compared with the modal survey of the CART0 wind turbine conducted at the National Wind Technology Center [5]. Our simulations are compared with their rotor being in a vertical azimuth configuration. To summarize, table 1 shows a comparison between the experimental modal survey of the CART0 wind turbine and the results obtained in this work. A good matching between the results and the modal survey is observed with reasonable error.

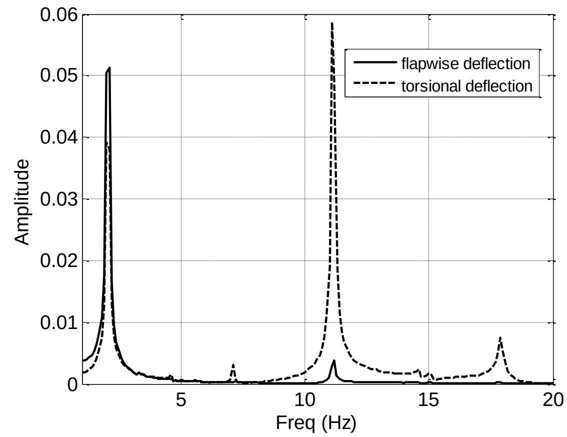

Figure 3. Blade flapwise and torsional deformation spectrum

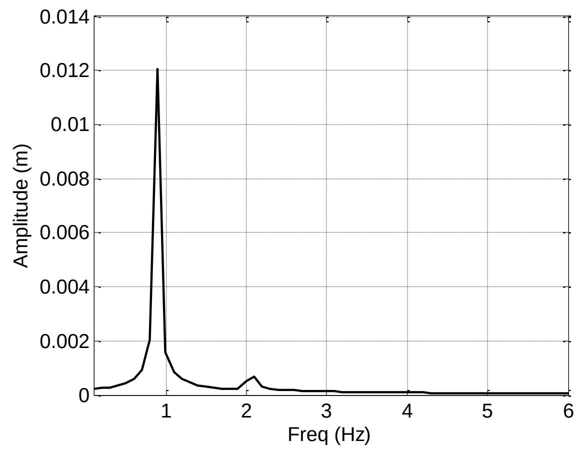

Figure 4. Tower fore-aft deformation spectrum

Table 1. Comparison of results from the Modal Survey and MBDyn

Modeshape Description	Modal Survey Freq. HZ	MBDyn Freq. HZ	Error %
1st tower fore-aft bending	0.858	0.898	4.6 %
1st tower lateral bending	0.877	0.898	2.4 %
1st flap wise	2.06	2.096	1.7 %

5 Steady Inflow Analysis

In this aeroelastic simulation, constant wind field with vertical shear inflow at 12m/s is applied. The vertical wind shear is defined by the hub height wind speed conformed to the power law shear profile shown in Eq. (12). It is used to determine the wind speed V_z at any height, z, based on the hub height, z_{hub}, and hub height wind speed, V_{hub}.

$$V_z = V_{hub}(z/z_{hub})^{\alpha} \quad (12)$$

Typically, the value of α is 0.1 for a sand terrain [10]. The displacements of the blade tip in a frame attached to the tower base are shown in Figure 5 and Figure 6.

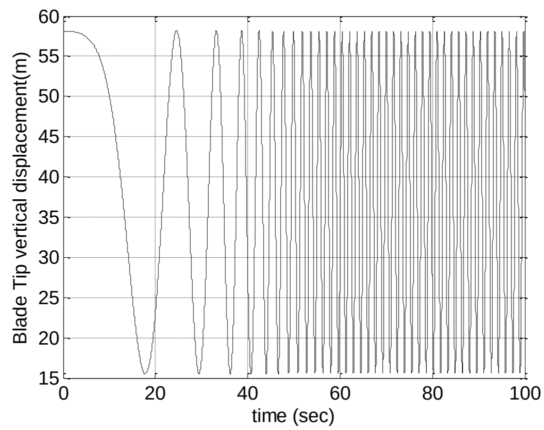

Figure 5. Blade tip vertical displacement

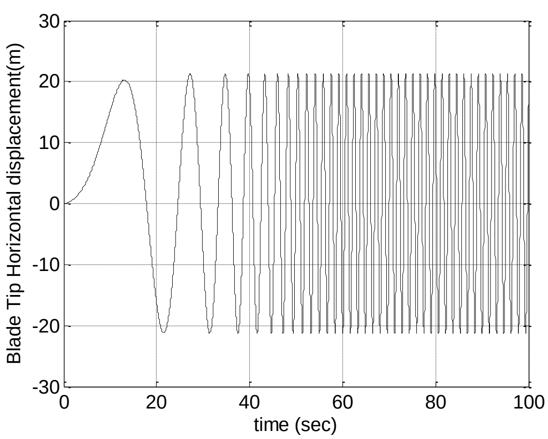

Figure 6. Blade tip horizontal displacement

Figure 5 shows that the vertical displacement of the blade tip is within 15.61 m and 58.14 m, which is the real physical range based on the previously mentioned blade and tower dimensions. Figure 6 shows that the horizontal displacement of the blade is again within the real physical range. The flapwise and edgewise deformations of the blade tip expressed in the blade root frame are shown in Figure 7 and Figure 8.

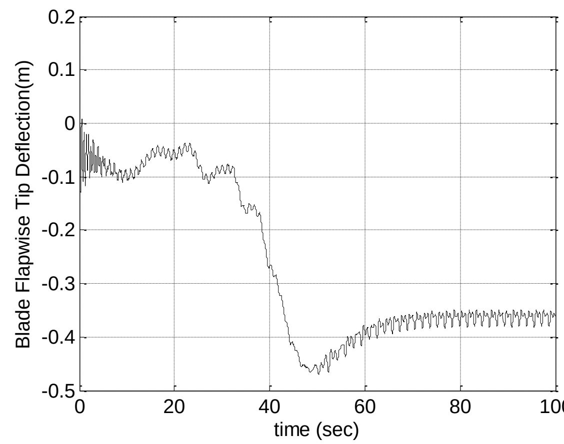

Figure 7. Blade flapwise deformation

Figure 7 shows a steady deformation of about 0.38 m backwards which is due to the steady inflow. The oscillations around this mean value is composed of two frequencies namely that due to the wind shear profile as well as that of the tower fore-aft oscillations.

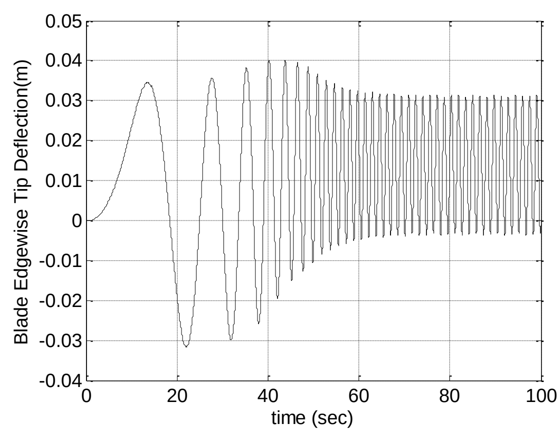

Figure 8. Blade edgewise deformation

From figure 8, it can be realized that the order of magnitude of the edgewise deformation is smaller than that of the flapwise, which is expected since the bending stiffness in the edgewise direction is higher than that in the flapwise direction.

The torsional deflection of the blade tip is shown in Figure 9. The magnitude of the steady-state response of the torsional oscillations is about -0.005 degrees which is considered to be negligible.

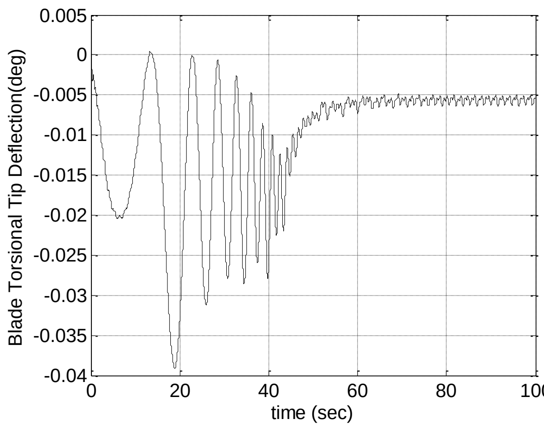

Figure 9. Blade torsional tip deformation

The wind turbine generator power is shown in Figure 10. A couple which is a quadratic function of the rotor angular velocity is applied at the rotor horizontal revolution hinge to counteract the aerodynamic torque.

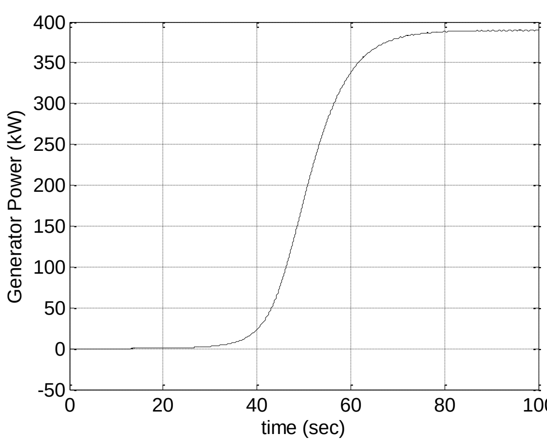

Figure 10. Generator power

For the given wind profile the wind turbine steady-state output power is then calculated and reached almost 400 kW which is within the rated power of the selected turbine.

6 Random Inflow Analysis

Random wind with maximum amplitude of 12 m/s is then applied together with the power law wind profile. The responses of the bladewise, torsional and tower fore-aft deformation are shown in Figures 11, 12 and 13 respectively.

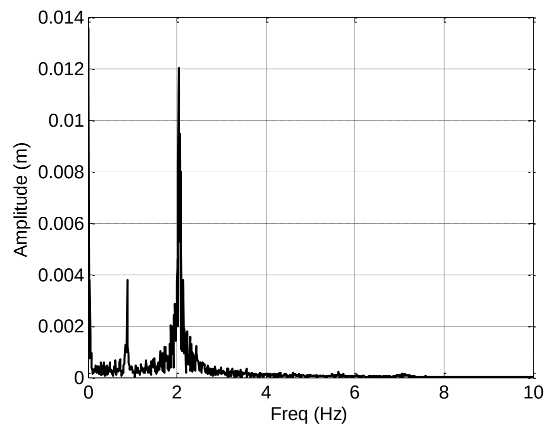

Figure 11. Blade flapwise deformation spectrum

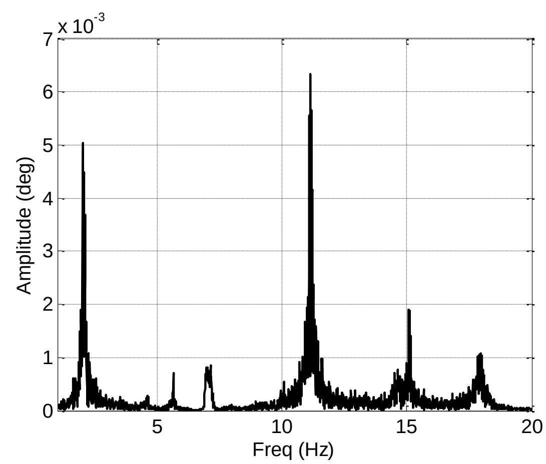

Figure 12. Blade Torsional deformation spectrum

A good agreement between the impulse response obtained earlier with that obtained from the random excitation is observed as expected. The torsional oscillation at the 2 Hz frequency, matching the frequency of the first bending mode, is mainly due to the coupling between the bending and the torsional modes which is also clear from Figure 3.

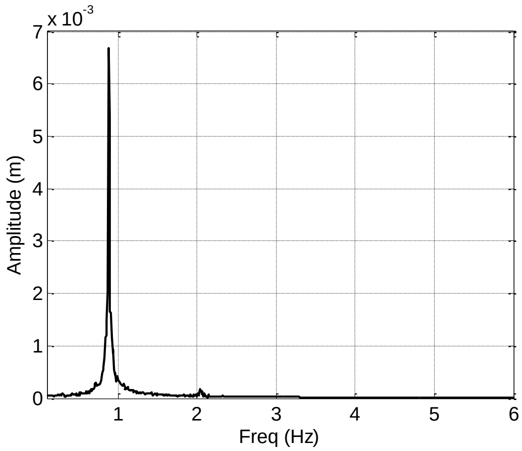

Figure 13. Tower fore-aft deflection spectrum

7 Conclusions

In this work, an aeroelastic analysis is implemented using a free multibody dynamic software. The modal analysis implemented by applying an impulsive wind field as well as that using random wind excitation showed good match with the modal survey carried out by the National Wind Technology Center. The output power of the turbine was also calculated for a steady wind inflow.

Acknowledgment

This work is funded by Science and Technology Development Fund (STDF) under project no. 1495. STDF is supported by the Egyptian State Ministry for Scientific Research.

References

[1] Meng, F., Masarati, P., Tooren, M. V. (2009), In *Proceedings* 47th AIAA Aerospace Sciences Meeting, Orlando, Florida, Free/Open Source Multibody and Aerodynamic Software for Aeroelastic Analysis of Wind Turbines.

[2] Lindenburg, C. (2003) "BLADMODE Program for Rotor Blade Mode Analysis," Ecn c–02-050.

[3] Meng, F., Pavel, M. D., Tooren, M. V. (2008), In *Proceedings* 46th AIAA Aerospace Sciences Meeting and Exhibit, Reno, Nevada, Aeroelastic Stability Analysis of Large Scale Horizontal Axis Wind Turbines Using Reduced Order System Identification Based on Flexible Nonlinear Multi-body Dynamics.

[4] Masarati, P., Morandini, M., Quaranta, G., and Mantegazza, P. (2003), In *Proceedings of* International Conference on Advances in Computational Multibody Dynamics, Lisboa, Portugal, *Open Source Multibody Analysis Software*, pp. 184–196.

[5] Stol, K. A. (2003), *Geometry and structural properties for the controls advanced research turbine (CART) from model tuning.* NREL/SR 500–32087, National Renewable Energy Laboratory.

[6] Manwell, J. F., McGowan, J. G., Rogers, A. L., (2002), *Wind Energy Explained Theory*. John Wiley and Sons Ltd

[7] http://www.nrel.gov/

[8] Cavagna, L., Fumagalli, A. , Masarati, P., Morandini, M., Mantegazza, P (2009), In *Proceedings* MULTIBODY DYNAMICS 2009, Warsaw, Poland, Real-Time Aeroservoelastic Analysis of Wind-Turbines by Free Multibody Software.

[9] Ghiringhelli, G., Masarati, P., Mantegazza, P. (2000), A multibody implementation of finite volume beams, *AIAA Journal,* 38*(1)*, 131–138.

[10] Bianchi, F., Battista, H., Mantz, R. (2007), *Wind Turbine Control Systems*. Springer.